Cell Death and Differentiation (2012) 19, 1152–1161

www.nature.com/cdd

# Retinoblastoma tumor-suppressor protein phosphorylation and inactivation depend on direct interaction with Pin1

F Rizzolio[1,6], C Lucchetti[1,2,7], I Caligiuri[1,2,7], I Marchesi[1,3], M Caputo[1,4], AJ Klein-Szanto[5], L Bagella[1,3], M Castronovo[6] and A Giordano[*,1,2,7]

**Inactivation of the retinoblastoma protein (pRb) by phosphorylation triggers uncontrolled cell proliferation. Accordingly, activation of cyclin-dependent kinase (CDK)/cyclin complexes or downregulation of CDK inhibitors appears as a common event in human cancer. Here we show that Pin1 (protein interacting with NIMA (never in mitosis A)-1), a peptidylprolyl isomerase involved in the control of protein phosphorylation, is an essential mediator for inactivation of the pRb. Our results indicate that Pin1 controls cell proliferation by altering pRb phosphorylation without affecting CDK and protein phosphatase 1 and 2 activity. We demonstrated that Pin1 regulates tumor cell proliferation through direct interaction with the spacer domain of the pRb protein, and allows the interaction between CDK/cyclin complexes and pRb in mid/late G1. Phosphorylation of pRb Ser 608/612 is the crucial motif for Pin1 binding. We propose that Pin1 selectively boosts the switch from hypo- to hyper-phosphorylation of pRb in tumor cells. In addition, we demonstrate that the CDK pathway is responsible for the interaction of Pin1 and pRb. Prospectively, our findings therefore suggest that the synergism among CDK and Pin1 inhibitors holds great promise for targeted pharmacological treatment of cancer patients, with the possibility of reaching high effectiveness at tolerated doses.**
*Cell Death and Differentiation* (2012) **19,** 1152–1161; doi:10.1038/cdd.2011.202; published online 10 February 2012

The retinoblastoma protein (pRb), the product of the *RB1* gene (i.e., the tumor-suppressor gene involved in hereditary and sporadic retinoblastoma pathogenesis), is mainly responsible for the control of cell proliferation via two different mechanisms. The first is based on the interaction between pRb and different chromatin-modifying enzymes: pRb interacts with histone deacetylases (HDACs) 1, 2, and 3, histone methylase SUV39H1, and chromatin-remodeling enzymes Brg1 and Brm, thus repressing gene expression.[1] The second mechanism involves pRb controlling the cell cycle through interaction with the E2F family of transcription factors[2] in a phosphorylation-dependent way: in early and mid G1, the protein complex D-type cyclins/CDK4,[6] whereas in late G1, cyclins E(A)/CDK2 gradually phosphorylate pRb. Hyperphosphorylated pRb releases E2F transcription factors and allows the expression of genes that mediate entry into the S phase.[3]

As pRb protein holds a central role in the cell cycle, its inactivation is necessary for enabling cancer cell proliferation. Different mechanisms of pRb inactivation have been described, although inactivation through phosphorylation is most common in human sporadic cancers. In this context, cyclin D1 overexpression induces CDK4/6 activation and thus pRb hyperphosphorylation.[4,5] In addition, the cyclin-dependent kinase (CDK) inhibitory partner, p16 protein (i.e., the product of the *CDKN2A* gene), is frequently inactivated through gene deletion or promoter hypermethylation.[6,7] In recent years, it has been discovered that Pin1 (protein interacting with NIMA (never in mitosis A)-1),[8] a peptidylprolyl isomerase that catalyzes *cis*-to-*trans* conformational switches of target proteins presenting the Ser/Thr-Pro motif, apparently increases the complexity of phosphoprotein regulation. In fact, Pin1 is overexpressed in most common tumors[9] and many of its target proteins that are involved in G0 and G1/S cell cycle control have an altered phosphorylation profile, including pRb.[10,11] Overall, these studies demonstrate that Pin1 is centrally involved in cell cycle control and in tumorigenesis as well.

Starting from the hypothesis that pRb could be a potential target of Pin1, our findings demonstrate a new mechanism of fine regulation of pRb phosphorylation during cell cycle

[1]Sbarro Institute for Cancer Research and Molecular Medicine, Center for Biotechnology, College of Science and Technology, Temple University, Philadelphia, PA, USA; [2]Department of Human Pathology and Oncology, University of Siena, Siena, Italy; [3]Department of Biomedical Sciences, Division of Biochemistry and Biophysics, National Institute of Biostructures and Biosystems, University of Sassari, Sassari, Italy; [4]Department of Pharmacology, University of Salerno, Fisciano, Salerno, Italy; [5]Department of Pathology, Fox Chase Cancer Center, Philadelphia, PA, USA; [6]Division of Experimental and Clinical Pharmacology, Department of Molecular Biology and Translational Research, National Cancer Institute and Center for Molecular Biomedicine, Aviano (PN), Italy and [7]Human Health Foundation, Terni and Spoleto (PG), Italy

*Corresponding author: A Giordano, Sbarro Institute for Cancer Research and Molecular Medicine, Center for Biotechnology, College of Science and Technology, Temple University, 1900 North 12th Street, Bio Life Sciences Building Suite 431, Philadelphia, PA 19122, USA. Tel: +1 215 204 9520; Fax: +1 215 204 9522; E-mail: giordano@temple.edu

**Keywords:** pRb phosphorylation; Pin1; CDK; cell cycle control

**Abbreviations:** Pin1, protein interacting with NIMA (never in mitosis A)-1; CDK, cyclin-dependent kinase; pRb, retinoblastoma protein; FACS, fluorescence-activated cell sorting; PIN1 KD, PIN1 knockdown; MEF, mouse embryonic fibroblast; PP1CA, protein phosphatase 1, catalytic subunit, $\alpha$ isozyme 1CA; MAPK, mitogen-activated kinase protein; AKT, v-akt murine thymoma viral oncogene homolog 1; HDAC, histone deacetylase; WB, western blot; qRT-PCR, quantitative real-time PCR

Received 17.6.11; revised 08.12.11; accepted 12.12.11; Edited by M Oren; published online 10.2.12

progression, where Pin1 works as a rheostatic controller. This concept raises new possibilities for improving drug intervention, through the design of effective pharmacological approaches for the treatment of pRb hyperphosphorylation-associated tumors.

## Results

**pRb phosphorylation and inactivation depend on Pin1.** To clarify the role of Pin1 in the RB/E2F pathway, we generated a *PIN1* knockdown (KD) T98G human glioblastoma multiforme (GM) cell line. These cells are easily synchronized and their cell cycle control depends on functional pRb.[12] Cells were infected with two *PIN1* shRNA lentiviruses (e.g., KD1 and KD2). Stable polyclonal cells underwent a $>90\%$ decrease in Pin1 protein level, compared with normal or scrambled shRNA-infected cells (Figure 1a). KD1 proved to be the most effective, and thus the most utilized in this study, except for some cases where KD2 was used to confirm the results. Then, we prepared *PIN1*KD1/HA*PIN1* (KD1 shRNA-resistant Pin1) and *PIN1*KD1/HA*PIN1*S76E[13] (catalytically inactive KD1 shRNA-resistant Pin1) cells and monitored the phosphorylation levels of pRb. Western blot (WB) analysis confirmed that in *PIN1* KD cells, the hypophosphorylated form of pRb was unchanged, whereas a reduced level of the hyperphosphorylated form was evident (Figure 1b). Overexpression of PIN1, but not the catalytically inactive form, restores pRb phosphorylation. The implications of these data were strengthened by using a phospho-specific antibody against pRb Ser780, a CDK4-specific target (Figure 1b). At the transcriptional level, no significant difference was observed in *RB1* RNA expression (Figure 1c), thus suggesting that Pin1 controls pRb phosphorylation via a posttranscriptional mechanism.

Loss of Pin1 in breast and mouse embryo fibroblast (MEF) cells is associated with cyclin D1 downregulation and pRb hypophosphorylation.[10,11] Starting from the observed phenotype in T98G cells, we analyzed the protein levels of the CDK/cyclin complexes controlling the G0 and G1/S transition phase of the cell cycle. WB analysis of cyclin D1, cyclin A, cyclin E, and the relative partners CDK2 and CDK4 demonstrated that no differences were detectable among normal, scrambled, and *PIN1* KD cells (Figure 1d). More recently, it has been demonstrated that Pin1 directly controls the stability of the CDK inhibitor p27 and indirectly controls that of p21.[14] To exclude any functional involvement of the CDK/cyclin complexes in the phenotype observed in *PIN1* KD cells, kinase assay experiments were carried out. CDK2, CDK4, and CDK6

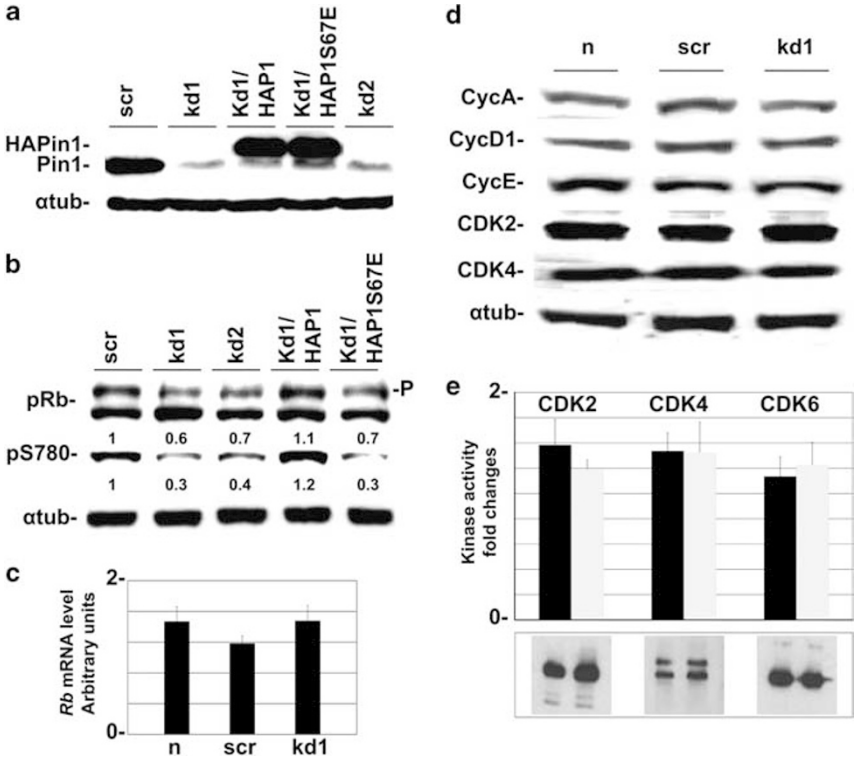


**Figure 1** T98G *PIN1* KD cells accumulate in G1. (**a**) WB analysis of T98G cells treated with scrambled (scr), *PIN1* (kd1 and kd2) shRNAs, and PIN1-overexpressing plasmids (HAP1 and HAP1S67E). The samples were analyzed with Pin1-specific antibody and normalized with $\alpha$-tubulin ($\alpha$-tub) antibody. (**b**) pRb is hypophosphorylated in *PIN1* KD cells. Overexpression of Pin1, but not the catalytically inactive form, restores pRb phosphorylation in *PIN1* KD cells. Cells were analyzed by WB with pRb and pRb-S780 phospho-specific antibodies. P, phosphorylation. The membrane was normalized with $\alpha$-tubulin. (**c**) Real-time PCR of pRb in *PIN1* KD cells was carried out as described in the Materials and Methods. Data shown represent mean $\pm$ S.D., $n=3$. (**d**) Normal (n), scrambled (scr), and *PIN1* knockdown (kd1) cells were analyzed by WB with different antibodies as specified on the left. (**e**) Kinase assay. (Upper panel) Total protein lysates were immunoprecipitated with indicated kinases and tested with ADP-glokinase assay (Promega) on scrambled (black) and *PIN1* KD (white) cells. (Lower panel) IP was loaded on WB and probed with the same antibody as in IP. Data shown represent mean $\pm$ S.D., $n=3$

activity remained substantially unchanged between control and *PIN1* KD cells (Figure 1e). Considering that pRb is actively dephosphorylated by PP1CA (protein phosphatase 1, catalytic subunit, $\alpha$ isozyme 1CA) during the M phase,[15] we therefore investigated possible links between Pin1 and PP1CA. WB analysis showed that the level of PP1CA was unaltered in *PIN1* KD cells (Supplementary Figure S1a), and no physical interaction between these two factors was evident by GST pull-down assay (Supplementary Figure S1b). The same results were obtained with PP2C$\alpha\beta$, which has been more recently shown to regulate the pRb family[16] (Supplementary Figure S1b).

Different authors report that loss of Pin1 in tumor cell lines and MEFs leads to defective cell proliferation.[10] We then evaluated the effect of Pin1 depletion on *in vitro* cell proliferation. As illustrated in Figure 2a, the *PIN1* KD cells proliferated less than scrambled cells (*$P<0.05$ and **$P<0.01$) Reintroduction of wild-type *PIN1* restores the proliferation defect. To define which phase of the cell cycle was altered, fluorescence-activated cell sorting (FACS) analyses were carried out. *PIN1* KD cells had more cells in G1 than control cells (65 *versus* 73%, Figures 2b and c). Again, reintroduction of wild-type *PIN1,* but not the catalytically inactive form, yields a normal cell cycle profile. *CDK4* KD cells (see Supplementary Figure S2a) were used as a positive control to show changes in cell cycle distribution of the cells (73% of cells in G1).

It was previously demonstrated that *PIN1* siRNA-targeted LNcaP and PC3 prostate cancer cells show significantly reduced cell proliferation rate, as well as anchorage-dependent and -independent colony formation, whereas increased cellular senescence and apoptosis are observed after stress stimuli.[17] FACS, caspase (Figure 2d), and $\beta$-galactosidase (Supplementary Figure S3) assays showed that the apoptotic pathway and senescence were not activated in *PIN1* KD cells as compared with controls. As a consequence, the cell morphology appeared essentially unchanged (Figure 2e).

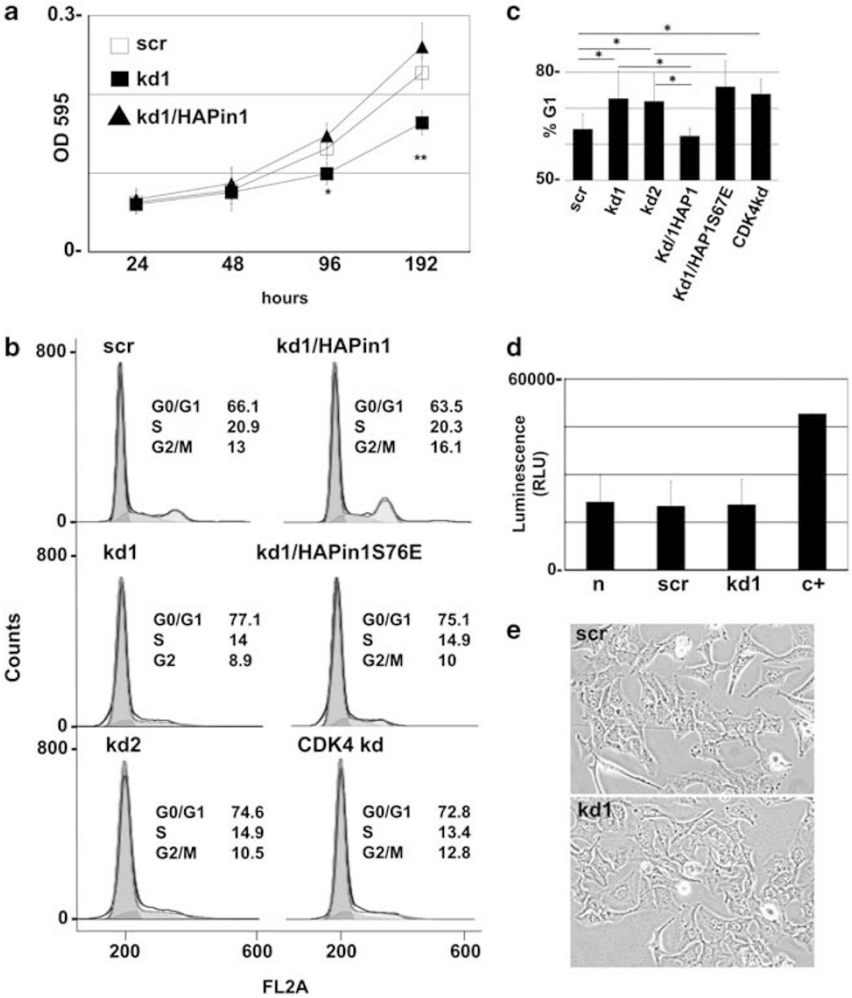


**Figure 2** CDK/cyclin complexes are unchanged and pRb is hypophosphorylated in T98G *PIN1* KD cells. (**a**) Proliferation assay showing that *PIN1* KD cells have reduced proliferation rate. Data shown represent mean ± S.D., $n=4$. OD, optical density; *$P<0.05$, **$P<0.01$. (**b**) A representative FACS analysis that shows *PIN1* KD cells (kd1 and kd2) have an increased number of cells in G1 compared with scrambled (scr) cells. Overexpression of Pin1, but not the catalytically inactive form, restores the phenotype of *PIN1* KD cells. (**c**) Average of six experiments as in (**b**). The percentage of G1 cells is shown (*$P<0.05$). (**d**) Caspase assay. Three independent experiments were analyzed: normal (n), scrambled (scr), and *PIN1* knockdown (kd1) cells; positive control cells treated with 1 $\mu$M doxorubicin for 18 h (c+). RLU, relative light unit per second. (**e**) Light microscope images at $\times$10 magnification showing no morphological difference between scrambled and *PIN1* KD cells

Collectively, these finding indicate that Pin1 controls cell proliferation by altering pRb phosphorylation without affecting CDK, CDK inhibitor, and protein phosphatase activity.

**Pin1 directly interacts with the pocket domain of pRb.** As the activity of CDK/cyclin complexes was not altered in *PIN1* KD cells, pRb still appeared hypophosphorylated. For this reason, we hypothesized that Pin1 can regulate pRb phosphorylation by direct interaction. pRb has more than 15 Ser/Thr-Pro motifs amenable to phosphorylation and thus potential targets of Pin1 (Supplementary Figure S4). T98G total-cell lysates were pulled down with GST-Pin1. Figure 3a demonstrates that pRb interacts with Pin1, mostly with its phosphorylated form. Indeed, it is widely accepted that Pin1 interacts with phosphorylated substrates. To test whether this was the case for pRb also, T98G cells were treated with shrimp alkaline phosphatase. In Supplementary Figure S5, the total input shows that such phosphatase treatment led to complete pRb dephosphorylation. In this setting, the interaction between pRb and GST-Pin1 was abrogated by shrimp alkaline phosphatase treatment. In addition, phospho-specific antibodies directed to Ser780 of pRb confirmed these findings (Supplementary Figure S5).

To provide evidence of the interaction between pRb and Pin1 *in vivo*, T98G cells were lysed, immunoprecipitated with anti-Pin1 antibody, and analyzed by WB using an anti-pRb antibody. The interaction appeared barely detectable in this setting (data not shown), and hence we decided to separate the nuclear and the cytoplasmic fractions. As shown in Figure 3b, the interaction was now clearly detectable, and primarily localized in the nucleus. As a negative control, the same experiment was carried out with *PIN1* KD cells and $\alpha$-tubulin and lamin A/C were used to assess the reliability of the nuclear/cytoplasmic preparation. These data clearly demonstrate that Pin1 and pRb form a macromolecular complex.

To demonstrate a direct interaction between pRb and Pin1, a FAR-western blot experiment was performed.[18] T98G cell lysate was immunoprecipitated with anti-pRb and transferred onto a nitrocellulose membrane. The membrane was then incubated with GST-Pin1 and probed with an anti-GST antibody. WB analysis revealed a band displaying the same apparent molecular mass of pRb (Figure 3c). To strengthen the implications of these data, T98G cells were lysed under denaturing conditions using a buffer containing SDS, treated with lambda phosphatase and, afterwards, proteins were immunoprecipitated using an anti-pRb antibody. The immunoprecipitated proteins were incubated with GST-Pin1 and then analyzed by WB using an anti-GST antibody. The results shown in Figure 3d thus confirm a direct interaction between phosphorylated pRb and Pin1 without intermediate factors.

The pRb protein consists of essentially three functional domains, that is, the N-terminal, the pocket, and C-terminal domain. Each of these domains is characterized by specific protein–protein interactions with other cellular factors. The pocket domain is highly conserved among all the three RB family members, pRb, p107, and pRb2/p130, and is involved in the interaction with the E2F family of transcription factors, thus mediating pivotal functional modulations in cell cycle regulation.[3] To investigate which among these three pRb domains was mainly involved in the interaction with Pin1,

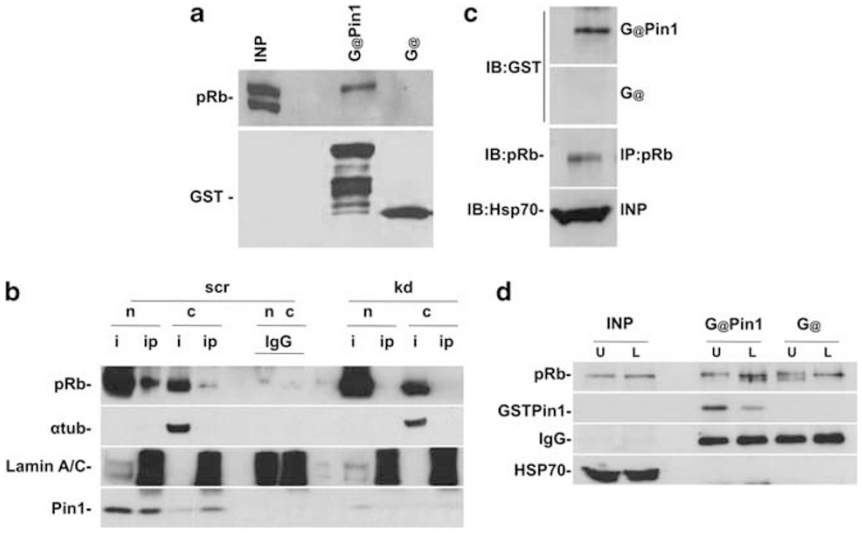


**Figure 3** *In vitro* and *in vivo* interaction between Pin1 and pRb. (**a**) GST-Pin1 interacts with pRb. It is noteworthy that the band corresponds to phospho-pRb. As a control, the membrane was probed with anti-GST antibody. (**b**) Pin1 interacts with pRb in the nucleus. Cells were immunoprecipitated with anti-Pin1 antibody, and analyzed by WB with anti-pRb antibody. As a control, *PIN1* KD cells were treated as normal cells. The interaction is evident in the nucleus. $\alpha$-Tubulin and lamin A/C antibodies were utilized to verify the nuclear/cytoplasmic fractions. The lamin A/C antibody yields a crossreacting nonspecific band in the IP samples, which is useful for controlling the loading of IgG lanes. n, normal; kd, *PIN1* knockdown; nuc, nucleus; cyt, cytoplasm; i, input; IP, immunoprecipitation; IB, immunoblot; IGg, immunoglobulin. (**c**) FAR-western blot experiment showing direct interaction between Pin1 and pRb. Proteins were immunoprecipitated with anti-pRb and transferred onto a nitrocellulose membrane. Membrane was incubated with GST or GST-Pin1 (see Materials and Methods). After washing, the membrane was probed with anti-GST or anti-pRb (diluted four times) as a control. (**d**) Denaturing IP, which demonstrates direct interaction between Pin1 and phosphorylated pRb. Lysates were treated with lambda phosphatase and immunoprecipitated with pRb antibody. The samples were incubated with GST-Pin1, washed, transferred onto the membrane, and probed with anti-GST antibody

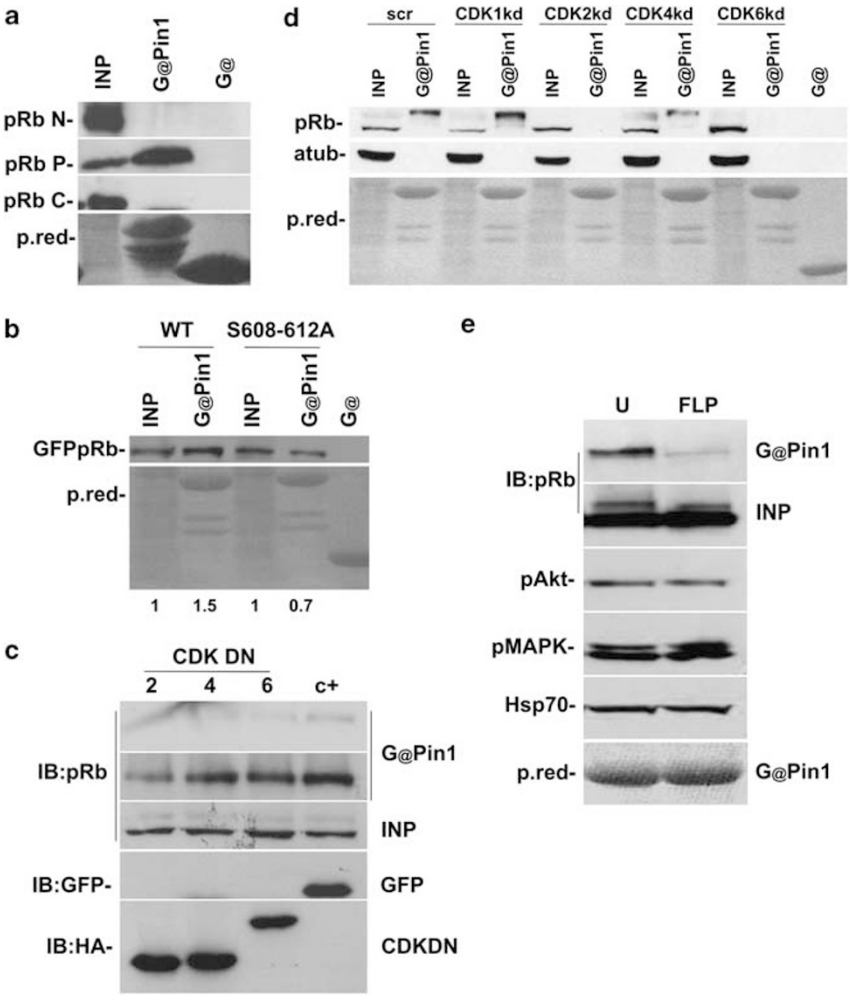


**Figure 4** CDKs allow Pin1 to interact with the spacer domain of pRb. (**a**) Pin1 interacts with the pocket domain of pRb. 293FT cells were transfected with expression vector coding for the HIS-MYC tag N-terminal, C-terminal, and pocket domains of pRb, and GST-pulled down with Pin1. The membrane was probed with anti-HIS antibody. (**b**) GFP-pRb-S608/612 were mutated to alanine, transfected in 293FT cells, and GST-pulled down with Pin1 and probed with anti-GFP. The signal intensity was quantified with the open source image analysis program ImageJ software (http://rsbweb.nih.gov/ij/). The pRb mutant interacts less with Pin1. (**c**) 293FT cells were transfected with CDK 2, 4, and 6 dominant-negative plasmids (in the top two rows, low and high exposure times are shown) or (**d**) with CDK 1, 2, 4, and 6 shRNAs and GST-pulled down with Pin1. The membrane was probed with anti-pRb. (**e**) T98G cells were treated with flavopiridol (FLP) and the lysate was GST-pulled down with Pin1. The membrane was probed with anti-pRb. The effect of FLP can be observed in the pRb INP lane, in which phosphorylation is strongly reduced. As a control, phospho-AKT, MAPK, and HSP70 were used

plasmid constructs expressing the N-terminal, pocket, or the C-terminal domains were expressed in 293FT cells. Lysates were precipitated with GST-Pin1. Figure 4a shows that the pRb pocket domain was able to interact with Pin1.

**Serine 608/612 in the pRb spacer domain are essential for pRb phosphorylation during cell cycle progression.** The spacer domain contains three different Ser/Thr-Pro motifs that could be targets of Pin1, namely, Ser567, Ser608, and Ser612. *In vivo* analysis of pRb phosphorylation has clearly demonstrated that only Ser608 and Ser612 are phosphorylated during the cell cycle.[19,20] Accordingly, alanin substitution of these two amino acids within the pocket structure produced a mutated polypeptide with a twofold decrease of binding affinity for Pin1 (Figure 4b). To verify whether this mutation affects other pRb-interacting proteins, HDAC1 and E2F1 were co-immunoprecipitated with wild-type pRb and pRbS608/612A (Supplementary Figure S6). We observed no difference in HDAC1 binding. Instead, E2F1 interacted more efficiently with pRbS608/612A as compared with wild-type pRb.

pRb is a major target of the CDK family of proteins and, specifically, Ser608 and 612 are targets of CDK2 and CDK4.[20] To assess whether CDKs played a role in the physical interaction between pRb and Pin1, 293FT cells were transfected with expression vectors coding for dominant-negative mutants of CDK2, CDK4, or CDK6.[21] After GST-Pin1 pull-down, WB analysis demonstrated that the dominant-negative CDK2 had the strongest competitive effects on pRb-Pin1 binding (Figure 4c). Although a reduced interaction between Pin1 and pRb was observed with the dominant-negative CDK4 and CDK6, the effect is less evident than CDK2. For this reason, we used the shRNA approach with which the effect on the CDK proteins can be directly assessed (Supplementary Figure S2b). Figure 4d shows that CDK2 and CDK6 had the strongest effect compared with CDK4. CDK1

had no effect (Figure 4d). To support these findings, cells were treated with flavopiridol, a potent CDK inhibitor. As shown in Figure 4e, our results reinforced the conclusion that CDK activities strongly increase the interaction between pRb and Pin1.

CDK proteins gradually phosphorylate pRb during the G0 and G1/S transition phase. The events that take part in driving this complicated mechanism are not entirely identified. On the basis of the evidence that CDKs strengthened Pin1–pRb interaction, and Pin1 was necessary for a complete pRb phosphorylation by CDKs, we have concluded that Pin1 may interact with pRb preferentially during G1. Accordingly, T98G cells were synchronized, released, and collected in G0, after 2 h (beginning of G1), 8 h (middle of G1), and arrested in G1/S (by adding HU).[16] GST pull-down experiments showed that Pin1 interacted with pRb in mid-G1, reaching the maximum binding level during G1/S (Figure 5a). At this point, as a consequence of the above-mentioned data, Pin1 is expected to increase the affinity between pRb and CDK/cyclin complexes. In fact, increased binding between the CDK4/cyclinD1 complex and pRb in the presence of Pin1 was demonstrated (Figure 5b). This binding is reduced by introducing the S608/612A mutation in the pRb protein (Figure 5c). The mechanism suggested by these results is that Pin1 boosts CDK-driven pRb phosphorylation.

Following our reasoning, if Ser608 and Ser612 are important for Pin1 binding, the mutant forms should impair Ser780 phosphorylation, as in *PIN1* KD cells. Figure 5d shows a decrease of Ser780 phosphorylation in pRb Ser608/612 mutants. Consequently, Ser608/612 should be phosphorylated before Ser780 during cell cycle progression. T98G cells were synchronized in G0, released, collected at different time points, and analyzed with pRb phospho-antibodies (Figure 5e and Supplementary Figure S7). Ser780 was phosphorylated after 13 h, in agreement with published results.[22] Ser608 showed the same kinetic profiling as Ser780. Ser612 was phosphorylated at the beginning of the cell cycle and a strong signal was detectable by WB 4 h after G0 release. All these data suggest that CDKs phosphorylate pRb Ser612, allowing Pin1 binding and, consequently, pRb hyperphosphorylation.

**pRb/Pin1 double KD cells proliferate like control cells.** To demonstrate that the decreased proliferation rate in T98G *PIN1* KD cells was mainly due to pRb, we used a

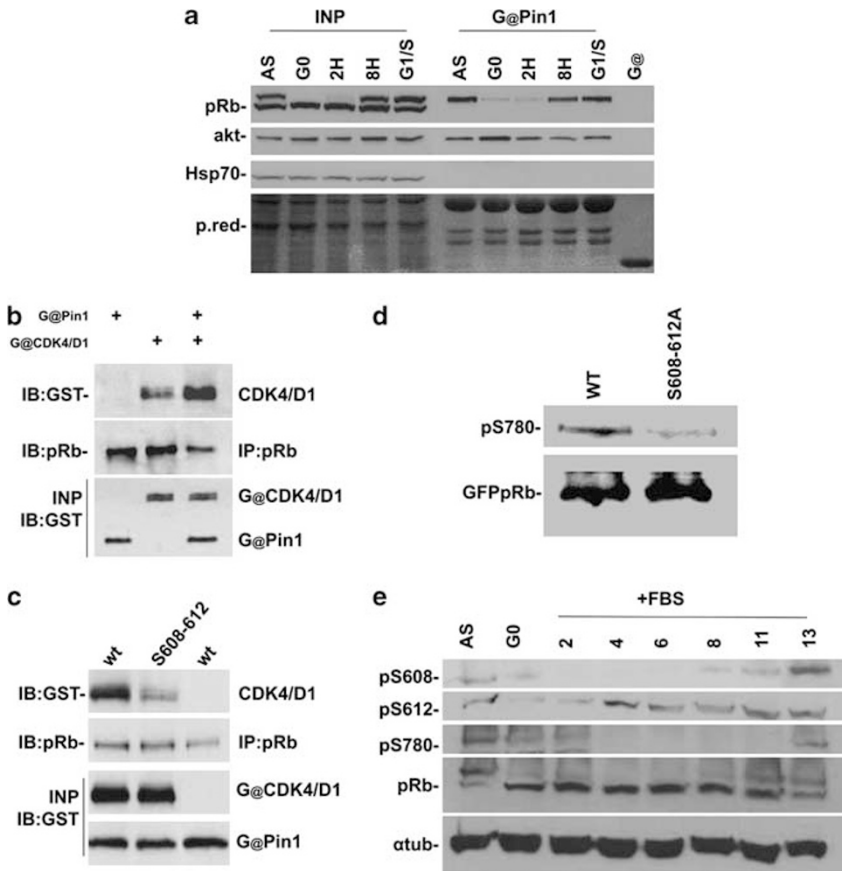


**Figure 5** Pin1 gradually interacts with pRb during G1 cell cycle. (**a**) T98G cells were serum starved and collected in G0, early-G1, mid-G1, and G1/S. WB shows Pin1 and pRb interaction starting in mid-G1 (8 h). AKT was used as a positive control of interaction (22). (**b**) Pin1 facilitates pRb and CDK4/cyclinD1 interaction. The protein lysates from T98G cells were immunoprecipitated with pRb antibody and incubated with GST-Pin1 or GST-CDK4/cyclinD1 or both. After washing, the proteins were loaded on polyacrylamide gel and the membrane was probed with anti-GST antibody. (**c**) GFP-pRb or GFP-pRbS608/612A were incubated with CDK4/CyclinD1 and Pin1 as in (**b**). The GFP-pRbS608/612A mutations affect the binding of CDK4/CyclinD1 to pRb. (**d**) 293FT cells were transfected with GFP-pRb or GFP-pRb-S608/612A and analyzed by WB with p-pRb-S780 and GFP antibodies. A reduction in Ser780 phosphorylation was evident in GFP-pRb-S608/612A mutants. (**e**) T98G cells were serum-starved, collected at different time points, and analyzed by WB with anti-phospho pRb-S608, -S612, and -S780, and pRb

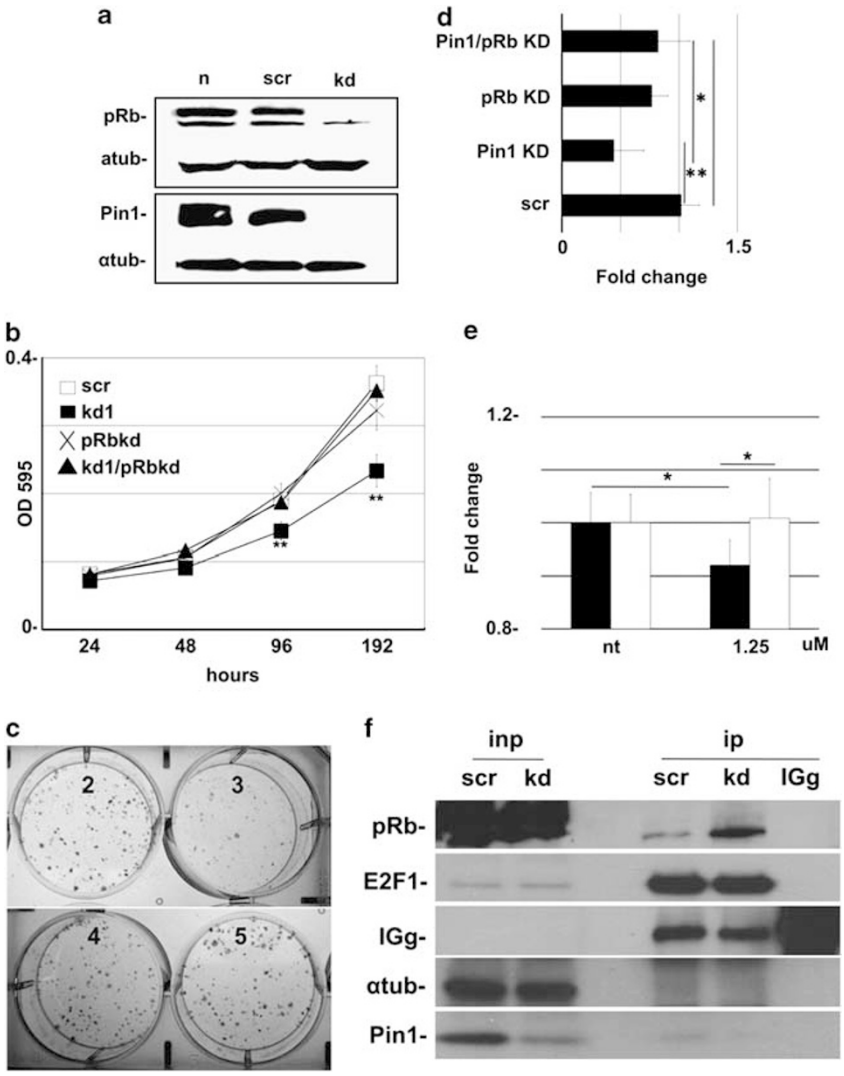


**Figure 6** pRb is the effector of Pin1 in G1/S cell cycle control. (**a**) WB analysis of *PIN1/RB1* KD T98G cells. (**b**) pRb is the effector of Pin1. Cell proliferation was assessed as in Figure 2a; $^{**}P<0.01$. (**c**) Colony-forming unit assay. Cells were grown for 2 weeks and stained with methylene blue. (2) Scrambled, (3) *PIN1* KD, (4) pRb KD, and (5) PIN1/pRb double KD cells. (**d**) Average of five experiments as in (**c**). $^{*}P<0.05$, $^{**}P<0.01$. (**e**) Scrambled (black) and pRb KD (white) cells were treated with indicated dose of Juglone ($^{*}P<0.05$). (**f**) T98G scrambled and *PIN1* KD cells were immunoprecipitated with E2F1 antibody. In *PIN1* KD cells, there is more interaction between pRb and E2F1

specific shRNA directed to pRb[23,24] (Figure 6a). A cell growth curve assay illustrated that *PIN1* KD cells proliferated at a lower rate than controls, whereas *PIN1/RB1* double KD cells proliferated at the same rate as scrambled cells (Figure 6b). *RB1* KD cells proliferated normally, as previously observed in other cell lines.[25] These data reveal that in T98G cells, pRb was the major target of Pin1 in controlling the cell cycle, without affecting CDK/cyclin protein complexes. To further sustain these data, we analyzed the proliferation rate of T98G *PIN1* KD cells by colony-forming unit assay. Figure 6c shows a representative experiment, whereas Figure 6d displays the average of five independent experiments, which show that the *PIN1* KD phenotype was rescued in the double *PIN1/RB1* KD cells. In order to prove and validate the shRNA experiments, we treated the *RB1* KD T98G cells with Juglone, a potent Pin1 inhibitor, at a nontoxic dose (Supplementary Figure S8). At very low concentration (1.25 $\mu$M), Juglone inhibited the proliferation of T98G scrambled cells, without affecting the proliferation rate of *RB1* KD cells (Figure 6e).

Finally, we tested the expression level of some pRb/E2F target genes in *PIN1* KD cells. Quantitative real-time PCR (qRT-PCR) presented in Supplementary Figure S9 demonstrated that *c-MYC* and *POLA* genes were downregulated. Co-immunoprecipitation experiments confirmed that in T98G *PIN1* KD cells, E2F1 interacts more efficiently with pRb than in scrambled cells (Figure 6f). These data confirmed that the pRb/E2F pathway in *PIN1* KD T98G cells was responsible for the observed reduced rate of proliferation.

**pRb phosphorylation depends on Pin1 in different cancer cells.** To extend the results obtained with the T98G cell line, we analyzed ovarian and breast cancer cells. A2780 (data not shown), OVCAR3, and MCF7 cells

were infected with *PIN1* shRNA and analyzed by WB. Similarly, in *PIN1* KD T98G cells, hypophosphorylated pRb was found in these *PIN1* KD cell lines, as shown in Figure 7a and Supplementary Figure S10. Kinase assay confirmed that, in OVCAR3 cells, CDK2, CDK4, and CDK6 activity was unchanged. In MCF7 cells, there was a decrease in CDK4 activity and an increase in CDK6 activity (Figure 7b). Our data are in agreement with previously published data, which demonstrate a decreased cyclin D1 expression,[11] and a reasonable decrease in CDK4 activity in breast cancer cells. Accordingly, with GST pull-down experiments, we demonstrated that pRb interacts with Pin1 in MCF7 and OVCAR3 cells also (Figure 7c). As OVCAR3 cells showed the same regulatory mechanism between Pin1 and pRb in T98G cells, we analyzed the cell cycle profile of these cells.

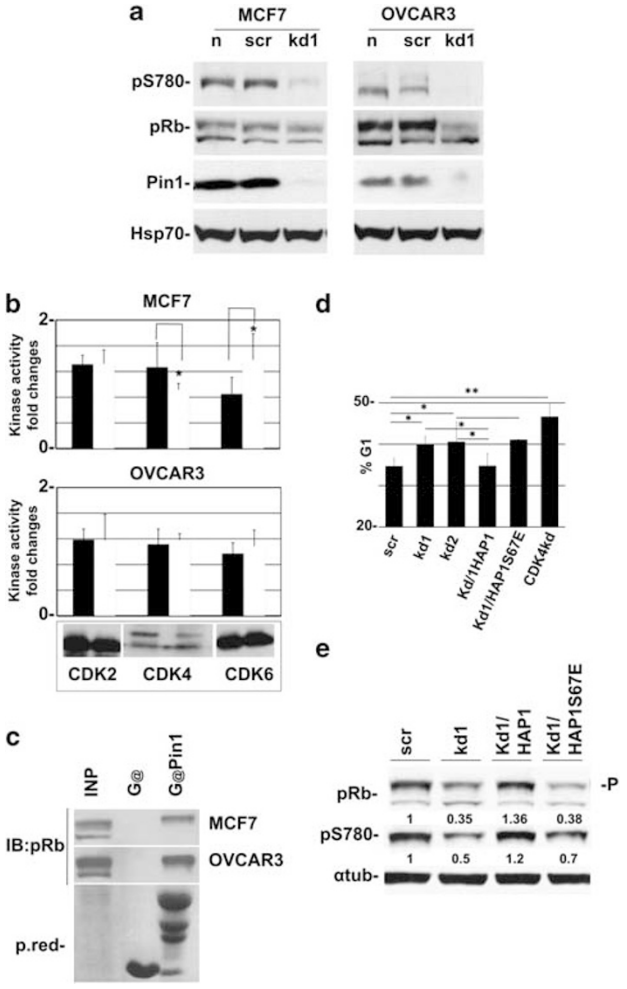


**Figure 7** Pin1 controls pRb phosphorylation in different cancer cells. (**a**) MCF7 and OVCAR3 *PIN1* KD cells showed hypophosphorylated pRb as in T98G cells. WB was stained with anti-Pin1, anti-p-pRb-S780, and anti-pRb. (**b**) Kinase assay performed as in Figure 1e. CDK/cyclin complexes were immunoprecipitated from MCF7 and OVCAR3 lysate cells (*$P<0.05$, **$P<0.01$). (**c**) GST-Pin1 interacts with pRb in MCF7 and OVCAR3 cells. (**d**) FACS analysis of OVCAR3 cells as in Figure 2c. (**e**) pRb is hypophosphorylated in *PIN1* KD OVCAR3 cells. Overexpression of Pin1, but not the catalytically inactive form, restores pRb phosphorylation in *PIN1* KD cells. Cells were analyzed by WB with pRb and pRb-S780 phospho-specific antibodies. P, phosphorylation. The membrane was normalized with $\alpha$-tubulin

Figure 7d shows that the loss of Pin1 has the same effect on G1 cells as in T98G cells. In addition, overexpression of wild-type Pin1, but not the catalytically inactive Pin1, in KD1 cells restores the phosphorylation level of pRb protein (Figure 7e).

## Discussion

pRb is gradually phosphorylated during cell cycle progression from G0 to G1/S phase, thereby allowing the expression of genes required for DNA synthesis and cell cycle progression. This process is regulated by a strict mechanism that results from the equilibrium between kinase and phosphatase activity.[26] Gain of function of the former or loss of function of the latter is commonly found in human cancers, leading in turn to pRb hyperphosphorylation, and its consequential functional inactivation.[27,28] The sequence of molecular events that triggers pRb phosphorylation during early, mid, and late G1 is not well known.

By investigating the cofactors that regulate this process, we propose a new model for pRb phosphorylation. Combining the published data with our new findings, we suggest the new model shown in Figure 8. At the beginning of G1, CDK2 and/or CDK4/6 phosphorylate pRb-Ser608/612, thus allowing the interaction with Pin1. The pRb isomerization done by Pin1 is essential for further phosphorylation of pRb and consequent inactivation. In turn, the Pin1-pRb complex releases E2F transcription factors, allowing for the expression of the S-phase entry gene. Here we propose the occurrence of a mechanism, elicited by Pin1, selectively boosting CDK-driven pRb phosphorylation.

Importantly, we have identified the critical motif that controls pRb phosphorylation. By interacting in the spacer domain, Pin1 allows pRb to achieve complete phosphorylation, as demonstrated by WB with pan-pRb and p-pRb-S780 antibodies, and appears to facilitate CDK4/cyclinD1 binding to pRb. Interestingly, recent studies suggest that phosphorylation at pRb-Ser608/612 promotes an intramolecular association between a conserved sequence in the flexible pocket linker and the pocket domain of pRb that occludes the E2F transactivation domain binding site.[29] This finding opens up a new possibility for a role of Pin1 as a scaffold protein that inhibits the interaction between pRb and the E2F factors.

Finally, the proliferation defect in *PIN1* KD cells can be specifically rescued by knocking down the pRb protein, thus

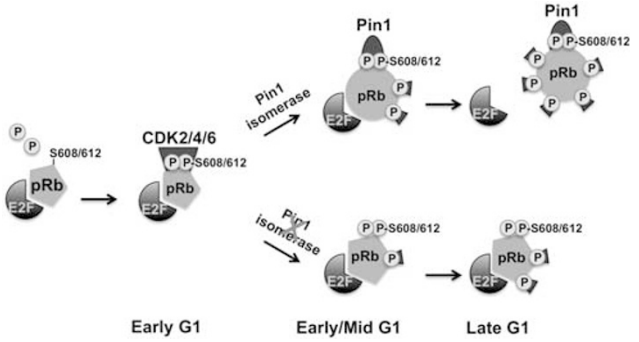


**Figure 8** A boosting model of Pin1–pRb interaction. See the Discussion section for description

highlighting pRb as a major target of Pin1 to control the G1/S cell cycle transition. However, some pRb/E2F target genes appeared downregulated in *PIN1*-deficient cells. Among them, the *c-MYC* proto-oncogene is found implicated in many tumors, and its overexpression can elicit cell transformation.[30]

Unlike the effects seen in prostate cancer cells and in neuronal cells,[8,17,31] we observed an increased number of *PIN1* KD T98G GM cells in G1 without a parallel increase in apoptotic or senescent cells, suggesting a cell-specific function of Pin1 in different pathways that control the equilibrium between growth, survival, and death.

In summary, we have identified a new mechanism for pRb inactivation, independent from CDKs and phosphatases. By altering pRb accessibility, Pin1 modifies the activity of CDKs. In such a context, Pin1 thus represents a new therapeutic target that, alone or in combination with CDK inhibitors, may provide a means to limit cancer cell growth via negative modulation of pRb phosphorylation. In addition, it is worth noting that *Pin1* KO mice develop normally;[24] this is very interesting from a therapeutic point of view. Most of the normal tissues that can develop tumors with high incidence, like prostate, lung, and colon, appear unaffected. Moreover, loss of PIN1 in normal human fibroblasts does not show any significant phenotype.[17] These results suggest that Pin1 could be crucial for tumor cells, and at least partially dispensable in normal cells. Different research groups are currently developing Pin1 small-molecule inhibitors, whose efficacy in anticancer therapy should be tested *in vivo*.[32–34]

Furthermore, we have found that the other two members of the pocket protein family, namely p130/pRb2 and p107, are substrates of Pin1. As in T98G cells the Pin1 and pRb interaction plays a major role in the G1/S cell cycle control, it would be interesting to analyze Pin1, pRb2/p130, and p107 in other cancer cells or other physiological processes.

Our study presents, for the first time, a new, detailed mechanism of pRb phosphorylation and suggests a novel approach of treating cancer patients by utilizing Pin1 inhibitors in combination with or without CDK inhibitors.

## Materials and Methods

**Cell culture assays and lentiviral production.** Cells were purchased from American Type Culture Collection (ATCC) (Manassas, VA, USA). For cell synchronization experiments, T98G cell growth was arrested by contact inhibition and serum starvation for 48 h. For G1/S enrichment, cells were split and grown in DMEM, 10% FBS in 2 $\mu$M hydroxyurea for 24 h as described.[35] Drug treatments were carried out with 100 nM Flavopiridol (Sigma-Aldrich, St. Louis, MO, USA) for 16 h. To generate knockdown cells, lentiviral particles were produced as described (http://www.broadinstitute.org/genome_bio/trc/publicProtocols.html). Briefly, $1 \times 10^6$ 293FT cells (Invitrogen, Carlsbad, CA, USA) were transfected with 2.25 $\mu$g of PAX2 packaging plasmid, 0.75 $\mu$g of PMD2G envelope plasmid, and 3 $\mu$g of pLKO.1 hairpin vector utilizing 30 $\mu$l of Fugene HD (Roche, Indianapolis, IN, USA) on 10 cm plates. Polyclonal populations of transduced cells were generated by infection with 1 MOI (multiplicity of infectious units) of shRNA lentiviral particles. At 3 days post infection, cells were selected with 2 $\mu$g/ml puromycin (Sigma-Aldrich) for 1 week.

**Plasmid construction and antibodies.** shRNA plasmids for pRb (SHCLNG-NM_000321), PIN1 (SHCLNG-NM_006221), CDK1 (SHCLNG-NM_001786), CDK2 (SHCLNG-NM_001798), CDK4 (SHCLNG-NM_000075), and CDK6 (SHCLNG-NM_001259) were purchased from Sigma-Aldrich. Scrambled shRNA (Addgene plasmid 17920), psPAX2 packaging (Addgene plasmid 12260), pMDG.2 envelope (Addgene plasmid 12259), CDK2 (Addgene plasmid 1885), CDK4 (Addgene plasmid 1877), and CDK6 (Addgene plasmid 1869) dominant-negative plasmids, and GFP-pRb (Addgene plasmid 16004) were purchased from non-profit plasmid repository Addgene (www.addgene.org). The pRb N-, P- and C-terminal domains were amplified (Supplementary Table S1) with PFU DNA Polymerase (Roche) and cloned in pcDNA6/myc-His (Invitrogen). HA*PIN1* was amplified from IMAGE:3941595 plasmid, digested with *Bam*HI/*NOT*I restriction enzyme, and cloned in pCDH-CMV-MCS-EF1-copGFP (SystemBio, Mountain View, CA, USA). Point mutations S576A and S608/612A on GFP-pRb and S67E on HA*PIN1* were performed by PCR (Supplementary Table S1) with Stratagene QuikChange II Site Directed Mutagenesis Kit (Stratagene, Santa Clara, CA, USA). All plasmids were sequence verified.

The antibodies PIN1 (600-401-A20), cyclin A (100-401-151), GFP (600-401-215) and GST (600_101_200) were purchased from Rockland Immunochemicals (Gilbertsville, PA, USA); pRb (sc-102), Hsp70 (sc-24), cyclin E (sc-481), HDAC1 (7872), CDK1 (sc-54), CDK2 (sc-163), CDK4 (sc-260), CDK6 (sc-177), E2F1 (sc-193, WB) IgG (sc-66931), pAKT (sc-7985R), p-pRb-S608 (sc-56174), PP1CA (sc-7482), and PP2C$\alpha\beta$ (sc-80665) were from Santa Cruz Biotechnology (Santa Cruz, CA, USA); E2F1 (05-379, IP) was from Millipore (Billerica, MA, USA); $\alpha$-tubulin (T-6074) was from Sigma-Aldrich; cycD1 (556470) was from BD Biosciences (Sparks, MD, USA); lamin A/C (2032), mitogen-activated kinase protein (MAPK; 9272), pMAPK (9101), v-akt murine thymoma viral oncogene homolog 1 (AKT; 9272), and p-pRb-S780 (9307) were from Cell Signaling (Boston, MA, USA); and p-pRb-S612 (AP3236a) was from Abgent (San Diego, CA, USA).

**Real-time PCR.** Real-time PCR was carried out essentially as described.[36] Total RNA was prepared from cells using the RNAeasy extraction kit (Qiagen, Valencia, CA, USA). Total RNA (1 $\mu$g) was reverse transcribed in a 20 $\mu$l reaction using M-MLV reverse transcriptase (Invitrogen). Primers are listed in Supplementary Table S1. The qRT-PCR was performed with SYBR Green PCR Master Mix (Roche) using a 7300 ABI instrument (Invitrogen). Samples were run in triplicates and the efficiency of each primer was calculated utilizing an internal standard control.[36] All values were normalized for *GAPDH*.

**FACS, cell proliferation, colony-forming unit, caspase 3/7, and $\beta$-galactosidase assays.** *FACS*: Cells were fixed by adding ice-cold 70% ethanol while vortexing. Fixed cells were stored at 4°C for at least 30 min and then washed once with PBS. Cells were stained with 10 $\mu$g/ml propidium iodide (Roche), 250 mg/ml RNase (Sigma-Aldrich) in PBS, and incubated at 37°C for 30 min in the dark. The percentage of cells in the different phases of the cell cycle was measured with a FACS Calibur instrument (Becton-Dickinson, Franklin Lakes, NJ, USA) and analyzed with FlowJo (Ashland, OR, USA) software. *Proliferation assay*: $2 \times 10^3$ T98G cells were plated in 96-well plates and stained with crystal violet at indicated times. The cell proliferation was evaluated by measuring the optical density at 540 nm. *Colony-forming unit assay:* $2 \times 10^3$ T98G cells were plated in a six-well plate and grown for 2 weeks. Cells were stained with methylene blue/ethanol and counted by two independent investigators. *Caspase 3/7 assay*: 10 $\mu$g/10 $\mu$l of protein was incubated with 10 $\mu$l of caspase 3/7 Glo assay (Promega, Madison, WI, USA) for 1 h at room temperature. *$\beta$-Galactosidase assay*: Subconfluent T98G cells were treated as described.[37]

**FAR-western blot.** The procedure was done essentially as described.[38] Briefly, 3 mg of proteins was immunoprecipitated with 3 $\mu$g of pRb antibody. The samples were run on 7% acrylammide gel and transferred onto a nitrocellulose membrane. The membrane was incubated with 5 $\mu$g of GST or GST-PIN1 and, after denaturing and renaturing treatments, it was probed with anti-PIN1 antibody and anti-pRb antibody as the control. Total lysate (25 $\mu$g) was loaded onto the gel and probed with an anti-Hsp70 antibody.

**Kinase assay.** Detection of kinase activity was performed using Kinase Glo luminescence assay (Promega). In all, 1 mg of protein from total cell lysate was immunoprecipitated with 1 $\mu$g of CDK2, CDK4, and CDK6 antibodies, and IgG as the negative control. After overnight (ON) incubation at 4°C, Protein A/G agarose beads (Pierce, Rockford, IL, USA) were added, incubated for 3 h, and washed three times with lysis buffer. Beads were resuspended in 10 $\mu$l kinase reaction buffer (40 mM Tris-HCl, 20 mM $MgCl_2$, 0.1 mg/ml BSA, 0.2 mM ATP, and 2 mM DTT) and incubated for 30 min at RT with specific substrates (CDK4/6: p107 and CDK2: p53). The reaction was terminated by adding 10 $\mu$l ADP-GLO reagent for 40 min at RT and 10 $\mu$l kinase detection reagent for 5 min at RT. A total of 1 $\mu$l of mixture from each experiment was loaded and analyzed by WB with CDK-specific antibodies.

**GST pull-down assay.** For GST pull-down experiments, the IMAGE:3941595 clone was utilized to amplify the *PIN1* human gene with the oligonucleotide primers with *Bam*HI and *Eco*RI adaptor sequences, respectively (Supplementary Table S1). The PCR-generated products were ligated in the pGEX-2T plasmid for the prokaryotic expression vector (Stratagene). All plasmids were sequenced verified. GST proteins were produced as described.[39] A total of 1 mg of protein was pulled down with 10 $\mu$g of GST or GST-Pin1 in lysis buffer A (20 mM Tris-HCl, pH 8, 137 mM NaCl, 10% glycerol, 1% Nonidet P-40 (NP-40), and 2 mM EDTA). To dephosphorylate proteins, 1 mg of protein lysate was treated with 50 U of shrimp alkaline phosphatase for 1 h at 37°C or 1600 U of lambda (sc-200312A) phosphatase for 30 min at 30°C.

**Co-immunoprecipitation assay.** Subconfluent T98G cells were harvested and 2 mg of proteins were pulled down in lysis buffer A with 4 $\mu$g of antibody. *Nuclear/cytoplasmic fractions*: Proteins were prepared as follows: the cell pellet was resuspended in NP-40 lysis buffer (0.01 M Tris-HCl, 0.01 M NaCl, 0.003 M $MgCl_2$, 0.03 M Sucrose, and 0.5% NP-40) to prepare the cytoplasmic fraction. Then, nuclei were pelleted and resuspended in lysis buffer (20 mM Tris-HCl, pH 8.0, 137 mM NaCl, 10% glycerol, 1% NP-40, and 2 mM EDTA). A total of 1 mg of protein was immunoprecipitated, utilizing 4 $\mu$g of antibody. Then, 50 $\mu$g of total lysate and IP proteins was run on polyacrylamide gel and probed with indicated antibodies.

**IP in denaturing lysis buffer and *in vitro* binding.** A total of 1 mg of protein was resuspended in denaturing lysis buffer (1% SDS, 5 mM EDTA, 10 mM $\beta$-mercaptoethanol, and protease inhibitors) and heated at 95°C for 10 min. The lysate was sonicated and diluted 10 times with 1% Triton X-100. IP was carried out with 2 $\mu$g of specific antibody. An equal amount of IP was incubated in lysis buffer with 300 ng of purified GST proteins for 1 h at RT. CyclinD1/CDK4 was purchased from SignalChem (Richmond, BC, Canada).

**Statistical analysis.** Statistical analyses were performed using R software by applying unpaired Student's *t*-test. In cellular growth curve experiments, we applied the one-way ANOVA test.

### Conflict of Interest

The authors declare no conflict of interest.

**Acknowledgements**. We thank Drs. Olimpia Meucci, Sander van den Heuvel, Didier Trono, and David Sabatini for plasmids available at Addgene; Drs. Marco Paggi and Wolfgang Bohn for scientific discussion; Mr. Robert Fratamico and Ms. Marie Basso for manuscript editing, the Sbarro Health Research Organization, Associazione Italiana per la Ricerca sul Cancro and Human Health Foundation for its support.

1. Dunaief JL, Strober BE, Guha S, Khavari PA, Alin K, Luban J *et al.* The retinoblastoma protein and BRG1 form a complex and cooperate to induce cell cycle arrest. *Cell* 1994; **79**: 119–130.
2. Wu CL, Zukerberg LR, Ngwu C, Harlow E, Lees JA. In vivo association of E2F and DP family proteins. *Mol Cell Biol* 1995; **15**: 2536–2546.
3. Rizzolio F, Esposito L, Muresu D, Fratamico R, Jaraha R, Caprioli GV *et al.* RB gene family: genome-wide ChIP approaches could open undiscovered roads. *J Cell Biochem* 2010; **109**: 839–843.
4. Rizzolio F, Tuccinardi T, Caligiuri I, Lucchetti C, Giordano A. CDK inhibitors: from the bench to clinical trials. *Curr Drug Targets* 2010; **11**: 279–290.
5. Gillett C, Fantl V, Smith R, Fisher C, Bartek J, Dickson C *et al.* Amplification and overexpression of cyclin D1 in breast cancer detected by immunohistochemical staining. *Cancer Res* 1994; **54**: 1812–1817.
6. Rane SG, Cosenza SC, Mettus RV, Reddy EP. Germ line transmission of the Cdk4(R24C) mutation facilitates tumorigenesis and escape from cellular senescence. *Mol Cell Biol* 2002; **22**: 644–656.
7. Nuovo GJ, Plaia TW, Belinsky SA, Baylin SB, Herman JG. In situ detection of the hypermethylation-induced inactivation of the p16 gene as an early event in oncogenesis. *Proc Natl Acad Sci USA* 1999; **96**: 12754–12759.
8. Lu KP, Hanes SD, Hunter T. A human peptidyl-prolyl isomerase essential for regulation of mitosis. *Nature* 1996; **380**: 544–547.
9. Bao L, Kimzey A, Sauter G, Sowadski JM, Lu KP, Wang DG. Prevalent overexpression of prolyl isomerase Pin1 in human cancers. *Am J Pathol* 2004; **164**: 1727–1737.
10. You H, Zheng H, Murray SA, Yu Q, Uchida T, Fan D *et al.* IGF-1 induces Pin1 expression in promoting cell cycle S-phase entry. *J Cell Biochem* 2002; **84**: 211–216.
11. Ryo A, Liou YC, Wulf G, Nakamura M, Lee SW, Lu KP. PIN1 is an E2F target gene essential for Neu/Ras-induced transformation of mammary epithelial cells. *Mol Cell Biol* 2002; **22**: 5281–5295.
12. Paggi MG, Felsani A, Giordano A. Growth control by the retinoblastoma gene family. *Methods Mol Biol* 2003; **222**: 3–19.
13. Girardini JE, Napoli M, Piazza S, Rustighi A, Marotta C, Radaelli E *et al.* A Pin1/mutant p53 axis promotes aggressiveness in breast cancer. *Cancer Cell* 2011; **20**: 79–91.
14. Zhou W, Yang Q, Low CB, Karthik BC, Wang Y, Ryo A *et al.* Pin1 catalyzes conformational changes of Thr187 in p27Kip1 and mediates its stability through a poly-ubiquitination process. *J Biol Chem* 2009; **284**: 23980–23988.
15. Ludlow JW, Glendening CL, Livingston DM, DeCarprio JA. Specific enzymatic dephosphorylation of the retinoblastoma protein. *Mol Cell Biol* 1993; **13**: 367–372.
16. Purev E, Giordano A, Soprano DR, Soprano KJ. Interaction of PP2A catalytic subunit with Rb2/p130 is required for all-trans retinoic acid suppression of ovarian carcinoma cell growth. *J Cell Physiol* 2006; **206**: 495–502.
17. Ryo A, Uemura H, Ishiguro H, Saitoh T, Yamaguchi A, Perrem K *et al.* Stable suppression of tumorigenicity by Pin1-targeted RNA interference in prostate cancer. *Clin Cancer Res* 2005; **11**: 7523–7531.
18. Gianni M, Boldetti A, Guarnaccia V, Rambaldi A, Parrella E, Raska Jr I *et al.* Inhibition of the peptidyl-prolyl-isomerase Pin1 enhances the responses of acute myeloid leukemia cells to retinoic acid via stabilization of RARalpha and PML-RARalpha. *Cancer Res* 2009; **69**: 1016–1026.
19. Delston RB, Matatall KA, Sun Y, Onken MD, Harbour JW. p38 phosphorylates Rb on Ser567 by a novel, cell cycle-independent mechanism that triggers Rb-Hdm2 interaction and apoptosis. *Oncogene* 2010; **30**: 588–599.
20. Zarkowska T, Sally U, Harlow E, Mittnacht S. Monoclonal antibodies specific for underphosphorylated retinoblastoma protein identify a cell cycle regulated phosphorylation site targeted by CDKs. *Oncogene* 1997; **14**: 249–254.
21. van den Heuvel S, Harlow E. Distinct roles for cyclin-dependent kinases in cell cycle control. *Science* 1993; **262**: 2050–2054.
22. Boylan JF, Sharp DM, Leffet L, Bowers A, Pan W. Analysis of site-specific phosphorylation of the retinoblastoma protein during cell cycle progression. *Exp Cell Res* 1999; **248**: 110–114.
23. Michaud K, Solomon DA, Oermann E, Kim JS, Zhong WZ, Prados MD *et al.* Pharmacologic inhibition of cyclin-dependent kinases 4 and 6 arrests the growth of glioblastoma multiforme intracranial xenografts. *Cancer Res* 2010; **70**: 3228–3238.
24. Atchison FW, Capel B, Means AR. Pin1 regulates the timing of mammalian primordial germ cell proliferation. *Development* 2003; **130**: 3579–3586.
25. Sage J, Mulligan GJ, Attardi LD, Miller A, Chen S, Williams B *et al.* Targeted disruption of the three Rb-related genes leads to loss of G(1) control and immortalization. *Genes Dev* 2000; **14**: 3037–3050.
26. Hirschi A, Cecchini M, Steinhardt RC, Schamber MR, Dick FA, Rubin SM. An overlapping kinase and phosphatase docking site regulates activity of the retinoblastoma protein. *Nat Struct Mol Biol* 2010; **17**: 1051–1057.
27. Sablina AA, Hahn WC. SV40 small T antigen and PP2A phosphatase in cell transformation. *Cancer Metastasis Rev* 2008; **27**: 137–146.
28. Mumby M. PP2A: unveiling a reluctant tumor suppressor. *Cell* 2007; **130**: 21–24.
29. Burke JR, Deshong AJ, Pelton JG, Rubin SM. Phosphorylation-induced conformational changes in the retinoblastoma protein inhibit E2F transactivation domain binding. *J Biol Chem* 2010; **285**: 16286–16293.
30. Dominguez-Sola D, Ying CY, Grandori C, Ruggiero L, Chen B, Li M *et al.* Non-transcriptional control of DNA replication by c-Myc. *Nature* 2007; **448**: 445–451.
31. Lu PJ, Wulf G, Zhou XZ, Davies P, Lu KP. The prolyl isomerase Pin1 restores the function of Alzheimer-associated phosphorylated tau protein. *Nature* 1999; **399**: 784–788.
32. Hennig L, Christner C, Kipping M, Schelbert B, Rucknagel KP, Grabley S *et al.* Selective inactivation of parvulin-like peptidyl-prolyl cis/trans isomerases by juglone. *Biochemistry* 1998; **37**: 5953–5960.
33. Zhang Y, Daum S, Wildemann D, Zhou XZ, Verdecia MA, Bowman ME *et al.* Structural basis for high-affinity peptide inhibition of human Pin1. *ACS Chem Biol* 2007; **2**: 320–328.
34. Wu B, Rega MF, Wei J, Yuan H, Dahl R, Zhang Z *et al.* Discovery and binding studies on a series of novel Pin1 ligands. *Chem Biol Drug Des* 2009; **73**: 369–379.
35. Balciunaite E, Spektor A, Lents NH, Cam H, Te Riele H, Scime A *et al.* Pocket protein complexes are recruited to distinct targets in quiescent and proliferating cells. *Mol Cell Biol* 2005; **25**: 8166–8178.
36. Rizzolio F, Bione S, Sala C, Tribioli C, Ciccone R, Zuffardi O *et al.* Highly conserved non-coding sequences and the 18q critical region for short stature: a common mechanism of disease? *PLoS One* 2008; **3**: e1460.
37. Dimri GP, Lee X, Basile G, Acosta M, Scott G, Roskelley C *et al.* A biomarker that identifies senescent human cells in culture and in aging skin in vivo. *Proc Natl Acad Sci USA* 1995; **92**: 9363–9367.
38. Wu Y, Li Q, Chen XZ. Detecting protein-protein interactions by Far western blotting. *Nat Protoc* 2007; **2**: 3278–3284.
39. Bagella L, Sun A, Tonini T, Abbadessa G, Cottone G, Paggi MG *et al.* A small molecule based on the pRb2/p130 spacer domain leads to inhibition of cdk2 activity, cell cycle arrest and tumor growth reduction in vivo. *Oncogene* 2007; **26**: 1829–1839.

Supplementary Information accompanies the paper on Cell Death and Differentiation website (http://www.nature.com/cdd)